JOURNAL OF BACTERIOLOGY, Apr. 2009, p. 2340–2352 Vol. 191, No. 7
0021-9193/09/$08.00+0 doi:10.1128/JB.01377-08

Psychrobacter arcticus 273-4 Uses Resource Efficiency and Molecular Motion Adaptations for Subzero Temperature Growth▽†

Peter W. Bergholz,* Corien Bakermans,‡ and James M. Tiedje

NASA Astrobiology Institute Center for Genomic and Evolutionary Studies on Microbial Life at Low Temperature and Center for Microbial Ecology, Michigan State University, East Lansing, Michigan

Received 1 October 2008/Accepted 6 January 2009

Permafrost soils are extreme environments that exert low-temperature, desiccation, and starvation stress on bacteria over thousands to millions of years. To understand how *Psychrobacter arcticus* 273-4 survived for >20,000 years in permafrost, transcriptome analysis was performed during growth at 22°C, 17°C, 0°C, and −6°C using a mixed-effects analysis of variance model. Genes for transcription, translation, energy production, and most biosynthetic pathways were downregulated at low temperatures. Evidence of isozyme exchange was detected over temperature for D-alanyl-D-alanine carboxypeptidases (*dac1* and *dac2*), DEAD-box RNA helicases (*csdA* and Psyc_0943), and energy-efficient substrate incorporation pathways for ammonium and acetate. Specific functions were compensated by upregulation of genes at low temperature, including genes for the biosynthesis of proline, tryptophan, and methionine. RNases and peptidases were generally upregulated at low temperatures. Changes in energy metabolism, amino acid metabolism, and RNase gene expression were consistent with induction of a resource efficiency response. In contrast to results observed for other psychrophiles and mesophiles, only *clpB* and *hsp33* were upregulated at low temperature, and there was no upregulation of other chaperones and peptidyl-prolyl isomerases. *relA*, *csdA*, and *dac2* knockout mutants grew more slowly at low temperature, but a *dac1* mutant grew more slowly at 17°C. The combined data suggest that the basal biological machinery, including translation, transcription, and energy metabolism, is well adapted to function across the growth range of *P. arcticus* from −6°C to 22°C, and temperature compensation by gene expression was employed to address specific challenges to low-temperature growth.

Low-temperature environments constitute approximately 80% of Earth's surface, including the majority of the world's ocean and polar soils (40). Growth at low temperatures impacts every aspect of cellular life by decreasing the rate of molecular motions, including protein conformational changes, nucleic acid secondary structure dynamics, diffusion of substrates, and motion of membrane lipids (42). Microbes living at temperatures below the freezing point of water must also cope with increased solute concentrations resulting from solute exclusion during the freezing process, and their opportunities for dispersal are limited (D. Gilichinsky, presented at the Fourth International Symposium on Thermal Engineering and Science for Cold Regions, U.S. Army Cold Regions Research and Engineering Laboratory, 1993). In spite of these challenges, metabolism at subzero temperatures has been demonstrated for psychrophiles isolated from polar and temperate frozen environments, including sea ice, cryopegs, and permafrost soils (6, 11, 30).

Metabolic acclimation might be required for specific cellular systems to function at low temperature and can be manifested either as increased expression of genes in order to compensate for reduced biochemical reaction rates or differential expression of isozymes adapted to separate thermal ranges, as has been observed in fish and bacteria (35, 44). Gene expression studies of both psychrotolerant and strict mesophiles growing at suboptimal temperatures have detected increased expression of proteins for destabilization of nucleic acid secondary structures, maintenance of membrane fluidity, chaperones, uptake of compatible solutes, and energy metabolism (2, 36, 47). However, reports of the global modifications to metabolism necessary for growth of psychrophiles at temperatures below 0°C remain rare (4, 5). Analysis of the amino acid sequences and structures of psychrophilic enzymes has given rise to the flexibility concept, i.e., that a psychrophilic enzyme can exhibit increased catalytic activity at low temperature with limited loss of thermostability by adaptation for reduced numbers of stabilizing interactions between key amino acid residues (20, 40). Therefore, the extent to which a eurypsychrophile (a psychrophile capable of growth in a broad thermal range [19]) requires adjustments in gene expression to overcome cold inhibition of growth is unclear.

Psychrobacter arcticus 273-4 was isolated from Kolyma lowland permafrost sediments continuously frozen for 10,000 to 40,000 years (3, 50). Siberian permafrost imposes four continuous stressors on resident microbes, including stable temperatures of approximately −10°C, desiccation due to freezing, decreased nutrient availability, and low continuous levels of radiation from soil minerals (21). Ponder et al. showed that *P. arcticus* was capable of growth at temperatures below 0°C and exhibited increased proportions of unsaturated membrane fatty acids and modified substrate utilization profiles during growth at 4°C and −2.5°C (37). *P. arcticus* grows in an experimentally confirmed temperature range of −10°C to 28°C and

* Corresponding author. Present address: 709 Bradfield Hall, Department of Crop and Soil Science, Cornell University, Ithaca, NY 14853. Phone: (517) 449-5943. Fax: (607) 255-8615. E-mail: pwb49@cornell.edu.

† Supplemental material for this article may be found at http://jb.asm.org/.

‡ Present address: Department of Earth Sciences, Montana State University, Bozeman, MT.

▽ Published ahead of print on 23 January 2009.

in a salinity range from 10 mM to 1.3 M NaCl (3). Therefore, we consider *P. arcticus* 273-4 a model organism for heterotrophic growth when an organism's environment is frozen.

Here we report that *P. arcticus* 273-4 exhibits two states of growth metabolism at different temperatures, a fast-growth state at the optimal temperature (T_{opt}) (17°C) and a resource efficiency state at temperatures less than 4°C. Three hypotheses were the focus of the transcriptome analysis described here: (i) transcriptomes at low temperature would be more similar to each other than to the transcriptomes at T_{opt}s, (ii) genes for cold acclimation proteins, such as RNA and protein chaperones, fatty acid desaturase, and translation factors such as the factor encoded by *rbfA*, would be transcribed at higher levels during growth at low temperatures, and (iii) acetate metabolism and energy metabolism would be upregulated at low temperature to compensate for increased energy demand per generation. We also noted exchange of isozyme expression at different growth temperatures and used knockout mutants to test the role of this expression and two additional differentially expressed genes in temperature adaptation. To the best of our knowledge, this is the first report of transcriptome analysis during growth at a temperature below 0°C.

MATERIALS AND METHODS

Microarray characteristics and printing. The *P. arcticus* 273-4 microarray consists of 2,144 70-mer oligonucleotide probes (Operon, Huntsville, AL). Arrays were printed in duplicate on CMT-UltraGAPS slides (Corning, Corning, NY). Each array consists of 1,998 probes for *P. arcticus* genes, 12 random oligonucleotides with no sequence matching any gene in the probe database, 10 SpotArray oligonucleotide probes (Stratagene, La Jolla, CA) to assay spiked positive controls, and 10 cloned human sequences with no sequence identity to *P. arcticus* genes. Additional empty spots contained only 0.3× SSC printing buffer (1× SSC is 0.15 M NaCl plus 0.015 M sodium citrate).

Strains, media, and culture conditions. For all experiments, single colonies of *P. arcticus* 273-4 were used to inoculate primary cultures in marine broth (MB), which grew to an optical density at 600 nm (OD_{600}) of ≥0.8 at 4°C. MB consisted of 3% (wt/vol) sea salts (Sigma-Aldrich, St. Louis, MO), 5 g liter^{-1} tryptone (BD, Sparks, MD), and 1 g liter^{-1} yeast extract (Difco). A 1% (vol/vol) inoculum of the starter culture was transferred to 7 ml of acetate medium. Acetate medium contained 75 g liter^{-1} sea salts (Sigma-Aldrich), 50 mM morpholinepropanesulfonic acid (MOPS) buffer (Sigma-Aldrich), 20 mM sodium acetate (Baker), 5 mM NH_4Cl (Baker) (pH 7.0) with NaOH, 1 mM K_2HPO_4 (Baker), 1× Wolfe's vitamins, and 1× trace mineral mixture. The Wolfe's vitamin (1,000×) and trace mineral solutions were made as described by Kostka and Nealson (31).

P. arcticus 273-4 was acclimatized to acetate medium by two passages to an OD_{600} of ≥0.8 at 4°C with shaking at 150 rpm before inoculation into experimental samples. A 5-ml inoculum from the final starter culture of *P. arcticus* in acetate medium was introduced into 500 ml acetate medium in 300-cm^2 untreated and vent-capped Falcon tissue culture flasks. Cultures were allowed to grow without shaking at −6°C, 0°C, 17°C, or 22°C until they reached an OD_{600} between 0.09 and 0.25 (mid-exponential phase at all temperatures).

Cell harvesting, RNA extraction, and cDNA synthesis. When cultures reached mid-exponential phase, 25 ml of a culture was preserved with 2 volumes of RNAprotect bacterial reagent (Qiagen, Valencia, CA) which had been chilled to the growth temperature of the culture. Cells in RNAprotect were incubated at room temperature for 5 min and then pelleted by centrifugation in a Sorvall RC-5B centrifuge at 4°C. Cells were resuspended in 1 ml of room temperature RNAprotect and pelleted again by centrifugation in an Eppendorf 5417R centrifuge at 4°C. The supernatant was decanted, and the cell pellet was frozen at −80°C.

RNA extraction was performed according to the instructions of an RNEasy mini kit (Qiagen), with some modifications. Specifically, lysozyme digestion was carried out for 30 min. Following cell lysis using buffer RLT (Qiagen), 1 μl each of a twofold dilution series of SpotReport mRNAs (Stratagene) containing from 1 ng to 1 pg of RNA was added to the lysate as controls for RNA degradation during sample preparation. Purified RNAs were analyzed by gel electrophoresis in a 1× FA gel containing 0.67% formaldehyde and 1.2% agarose.

Three 5-μg aliquots of total RNA were denatured with 6 μg random hexamers (Invitrogen, Carlsbad, CA) in a 17.5-μl mixture for 10 min at 70°C and snap-cooled for 5 min on ice. Denatured total RNA mixtures were reverse transcribed to obtain amino-allyl labeled cDNAs by combining the total RNA mixture with 6 μl 5× First Strand synthesis buffer, 3 μl 0.1 M dithiothreitol, 1 μl RNaseOUT (Invitrogen), 1.2 μl 25× deoxynucleoside triphosphates (ratio of amino-allyl dUTP to dTTP, 3:2), and 2 μl Superscript II reverse transcriptase (Invitrogen). Amino-allyl dUTP was obtained from Ambion (Austin, TX). Reaction mixtures were incubated at 42°C overnight, and reactions were stopped by addition of 10 μl 0.5 M EDTA. RNA was hydrolyzed by incubation with 10 μl 1 M NaOH at 65°C for 15 min. RNA hydrolysis was neutralized with 10 μl 1 M HCl. Amino-allyl-labeled cDNAs were purified using the amino-allyl labeling protocol of The Institute for Genomic Research (TIGR) (26).

Microarray hybridization. Amino-allyl-labeled cDNAs were resuspended in 4.5 μl 0.1 M Na_2CO_3 (pH 9.0) for 10 min at room temperature and combined with 4.5 μl Cy3 or Cy5 *N*-hydroxysuccinamide ester in dimethyl sulfoxide (GE Biosciences, Piscataway, NJ). Dye incorporation reaction mixtures were incubated at 25°C for 1.5 h. Equal picomole nucleotide amounts of dye-labeled cDNA samples were hybridized such that the amount of neither Cy3 nor Cy5 exceeded 550 pmol. cDNAs were dried in a SpeedVac for 1.5 h. A hybridization mixture was prepared by resuspending cDNA pellets in 50 μl 5× SSC, 25% formamide, 0.1% sodium dodecyl sulfate (SDS), 0.1 mg ml^{-1} salmon testis DNA (Sigma-Aldrich).

Glass slide arrays were prehybridized by incubation in 5× SSC, 0.1% SDS, 0.1 mg ml^{-1} bovine serum albumin for 60 min at 49°C. Slides were then washed twice in room temperature 0.1× SSC for 5 min and twice for 30 s in sterile water. Prehybridized slides were then immediately dried by centrifugation for 3 min at 1,600 rpm in a Sorvall RT 6000D centrifuge with an H1000B hanging basket rotor. Lifterslips (22 by 60 mm; Erie Scientific, Portsmouth, NH) were washed in sterile water, followed by 100% ethanol, and dried under filtered forced air. The hybridization mixture was preheated to 95°C for 10 min and then pipetted onto each slide. Hybridization cassettes were sealed and incubated in a 49°C water bath with shaking at 30 rpm for 20 h.

Hybridizations were performed for all growth temperature comparisons with five biological replicates at each temperature. Hybridized slides were first washed in 2× SSC, 0.1% SDS for 5 min at 49°C. A second wash was performed twice in 0.1× SSC, 0.1% SDS at room temperature for 5 min. A third wash was performed four times in 0.1× SSC for 1 min. The final wash was in 0.01× SSC for 10 s. Washed slides were dried by centrifugation as described above. Slides were scanned using a Genepix 4000B scanner (Molecular Devices, Sunnyvale, CA). Images were analyzed using Genepix 6.0 software, and results were analyzed for quality using the marray and arrayQuality packages in R 2.3.0 (http://www.r-project.org/). Only slides passing the quality control analysis were included in the biological analysis.

The statistical significance of the temperature effect on gene expression was computed using two microarray analysis packages in R: R/MAANOVA 1.0 to determine statistical significance and LIMMA 2.7.10 to estimate pairwise differences in gene expression (43). In both cases data were normalized using regional (print tip) lowess normalization (12, 53). Normalized data were fitted to a mixed-effects analysis of variance (ANOVA) model with gene, dye, and temperature as fixed terms. Slide and biological replicate were random terms (13). F tests were carried out using the variance shrinking Fs statistic to determine the statistical significance of differential expression with 500 permutations to evaluate the distribution of Fs (14). Genes were considered differentially expressed if the *P* value was <0.01 after Benjamini-Hochberg *P* value adjustment for multiple-hypothesis testing (13). Pearson correlations between ANOVA temperature effect estimates for gene expression and temperature were calculated in R 2.5.10. The false discovery rate for the statistically significant genes was estimated by the method of Storey using the qvalue package in R (45).

Proteome. For analysis of the proteome, cells were harvested from the remaining 475 ml of the transcriptome sample culture and analyzed as described by Bakermans et al. (5). Briefly, samples were centrifuged at 10,000 × *g* in a Sorvall RC-5B refrigerated centrifuge at the culture temperature for 10 min. Supernatants were removed, and cell pellets were extracted with an equal volume of urea solubilization buffer. The denatured soluble proteins were recovered in the supernatants after centrifugation of the samples at 435,000 × *g* for 10 min. Samples were stored at −80°C until analysis by two-dimensional gel electrophoresis.

At the MSU Proteomics Facility, 240-μg aliquots of each sample were precipitated using chloroform-methanol (1:4). and the resulting pellets were resuspended in rehydration buffer containing 8 M urea, 4% (wt/vol) 3-[cholamidopropyl]-dimethylammonio]-1-propanesulfonate (CHAPS), 0.2% (vol/vol) carrier ampholytes, 50 mM dithiothreitol, and 0.2% (vol/vol) bromophenol blue to

obtain a final volume of 200 μl. Samples were incubated at room temperature for 30 min, and precipitates were removed by centrifugation at 21,000 × *g* for 5 min and subsequently applied to precast ReadyStrip IPG strips (11 cm; pH 3–10 NL; Bio-Rad) by passive rehydration (14 h at 20°C). Rehydrated strips were focused using a PROTEAN isoelectric focusing cell (Bio-Rad). The voltage was raised linearly to 250 V, kept at 250 V for 15 min, and then rapidly ramped to 8,000 V and kept at 8,000 V for 25,000 V · h. Strips were transferred into 3 ml of equilibration buffer (6 M urea, 2% [vol/vol] SDS, 20% [vol/vol] glycerol, 50 mM Tris HCl [pH 8.8]) containing 2% (wt/vol) dithiothreitol, incubated for 30 min at room temperature, placed into 3 ml equilibration buffer containing 2.5% (wt/vol) iodoacetamide, and incubated for 30 min at room temperature. Finally, strips were positioned on top of an 8 to 16% Tris-HCl precast Criterion gel (8.7 by 13.3 cm; Bio-Rad) and fixed in place with an agarose overlay (0.5% [wt/vol] agarose, 45 mM Tris-borate, 1 mM EDTA, 0.5% [vol/vol] bromophenol blue). Gels were run at a constant voltage of 120 V in a Criterion Dodeca cell (Bio-Rad) with running buffer (25 mM Tris, 192 mM glycine, 0.1% SDS) until the bromophenol blue ran to the bottom of the gel.

Protein spots were visualized by staining with ruthenium (II)-tris(bathophenanthroline) disulfonate. Gels were fixed for 2 h in 40% (vol/vol) methanol, 20% (vol/vol) acetic acid, which was followed by staining overnight in 20% (vol/vol) methanol, 10% (vol/vol) acetic acid with ruthenium (II)-tris(bathophenanthroline) disulfonate (20 μl/liter). Gels were washed twice for 15 min in 10% (vol/vol) acetic acid and then twice for 15 min in 5% (vol/vol) acetic acid. Gels were scanned using a Molecular FX scanner (Bio-Rad) at 100-μm resolution.

Gel images were analyzed using Image Master 4 (trial version) software available from the Swiss Institute of Bioinformatics as described by Bakermans et al. (5) to identify proteins with clear expression patterns. Ten protein spots that were upregulated at −6°C (the relative abundance at −6°C was more than twofold higher than that at 22°C) and 10 spots that were upregulated at 22°C were selected for identification by mass spectrometry at the MSU Proteomics Facility.

Genetics. Knockout mutants with mutations in *relA* (Psyc_0343), *dac1* (Psyc_0687), *dac2* (Psyc_0704), and *csdA* (Psyc_1082) were generated using the pJK100 suicide vector (15). Primers, plasmids, and strains used in this study are described in Table S1 in the supplemental material. Upstream flanking regions were amplified with primers containing BglII and NotI restriction sites at the 5′ ends of the forward and reverse primers, respectively. Downstream flanking regions were amplified with SacII and SacI sites appended to the 5′ ends of the forward and reverse primers, respectively. PCR products were digested with the restriction enzymes mentioned above and ligated into pJK100 using T4 DNA ligase (Invitrogen). The resulting plasmids were transformed into *Escherichia coli* WM3064 by electroporation.

P. arcticus 273-4 cultures used for conjugation were grown in Luria-Bertani (LB) broth at 22°C for 36 h. *E. coli* WM3064 containing the suicide vector for knockout was grown at 37°C in LB broth supplemented with 25 μg ml^{-1} kanamycin (Kan), 20 μg ml^{-1} tetracycline (Tet), and 100 μg ml^{-1} diaminopimelic acid overnight. Cells were combined using a ratio of 200 μl of the *E. coli* donor and either 200 μl or 800 μl of the *P. arcticus* 273-4 recipient, 100 μl was spot plated on LB agar containing 100 μg ml^{-1} diaminopimelic acid, and conjugation was allowed to proceed for 24 h at 22°C. Growth on spot plates was suspended in 1 ml LB broth. Putative conjugants (50 μl and 200 μl) were plated on LB medium containing 25 μg ml^{-1} Kan. Conjugants were allowed to grow for 72 h at 22°C. Putative knockouts were isolated on LB medium plates with 25 μg ml^{-1} Kan and screened for a Kan^r Tet^s phenotype. PCR screening of knockouts with primers annealing outside the target gene yielded the expected product size, as did screening of wild-type controls.

Mutant growth rate experiments. Representative isolates of the knockout mutants were grown in MB supplemented with 25 μg ml^{-1} Kan for 48 h at 22°C. Two subsequent rounds of culturing were carried out in acetate medium with 25 μg ml^{-1} Kan for 72 h.

Mutant growth rates were determined using 96-well plates. Eight replicates of each mutant were inoculated into 200 μl acetate medium in each well. Sixteen replicates of wild-type *P. arcticus* 273-4 were present on each plate along with 12 blank wells. Plates were incubated at 22°C, 17°C, 4°C, 0°C, and −2.5°C. An incubator failure prevented mutant growth assays at −6°C from being completed. OD_{600} data from which blanks were subtracted were collected using a SpectraMax M2 spectrophotometer (Molecular Devices). Average growth rates were calculated, and two-tailed *t* tests were performed to determine if the growth rates of wild-type *P. arcticus* and knockout strains were statistically different at a temperature. Strains were considered statistically different from the wild type if the *P* value was <0.05.

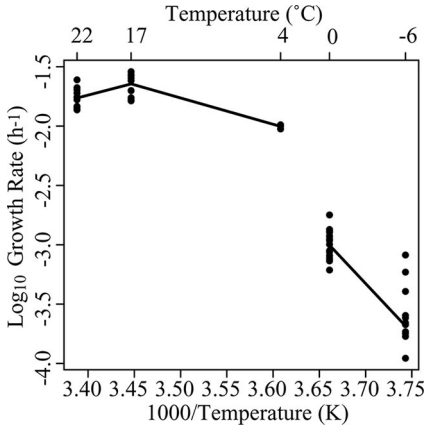

FIG. 1. Log-transformed growth rates plotted versus temperature. Temperature was transformed according to the Arrhenius equation. Celsius temperatures are indicated at the top. *P. arcticus* was grown at 22°C, 17°C, 4°C, 0°C, and −6°C. Trend lines were generated by lowess fitting to the data points over the following intervals: 22°C to 17°C, 17°C to 4°C, and 0°C to −6°C.

Microarray data accession number. Microarray data have been deposited in the Gene Expression Omnibus repository (http://www.ncbi.nih.nlm.gov/geo) under series accession number GSE12871.

RESULTS

Growth physiology changes with temperature. Acetate minimal medium was previously determined to support growth rates similar to those observed in complex media (data not shown), and this medium was expected to permit more reproducible expression analysis during exponential growth than complex media. Growth rate measurements were obtained for −6°C, 0°C, 4°C, 17°C, and 22°C in acetate medium. No stable growth was observed at temperatures higher than 22°C. Two growth states were observed by examination of the decrease in the growth rate over temperature for *P. arcticus* (Fig. 1). Whereas the decline in the growth rate over 10°C was 1.9-fold between 17°C and 4°C, the corresponding decline in the temperature range from 0°C to −6°C was 8.4-fold. Discontinuity between the growth rate trends at low and high temperatures was indicative of changes in growth physiology.

Transcriptome changes over temperature. Microarray analysis of mid-exponential growth in acetate medium at −6°C, 0°C, 17°C, and 22°C was performed to elucidate gene expression changes in response to temperature. Salt concentrations were kept constant in order to isolate the effect of changing temperature in this experiment. Mixed-model ANOVA identified 1,085 coding sequences that were significantly differentially expressed during growth at one or more temperatures with a corrected *P* value of <0.01. As determined by the method of Storey and Tibshirani (45), the false discovery rate for the 1,085 smallest genewise *P* values was 0.0025. Temperature comparison plots of the microarray results demonstrated that the transcriptomes at 0°C and −6°C were more similar to each other than to the transcriptomes at 22°C and 17°C (17 and 46 differentially expressed transcripts, respectively) (Fig. 2A and B). The largest number of differentially expressed genes, 562 genes (27% of the *P. arcticus* genome), was observed in the comparison of the data for −6°C and 17°C (Fig. 2F). For

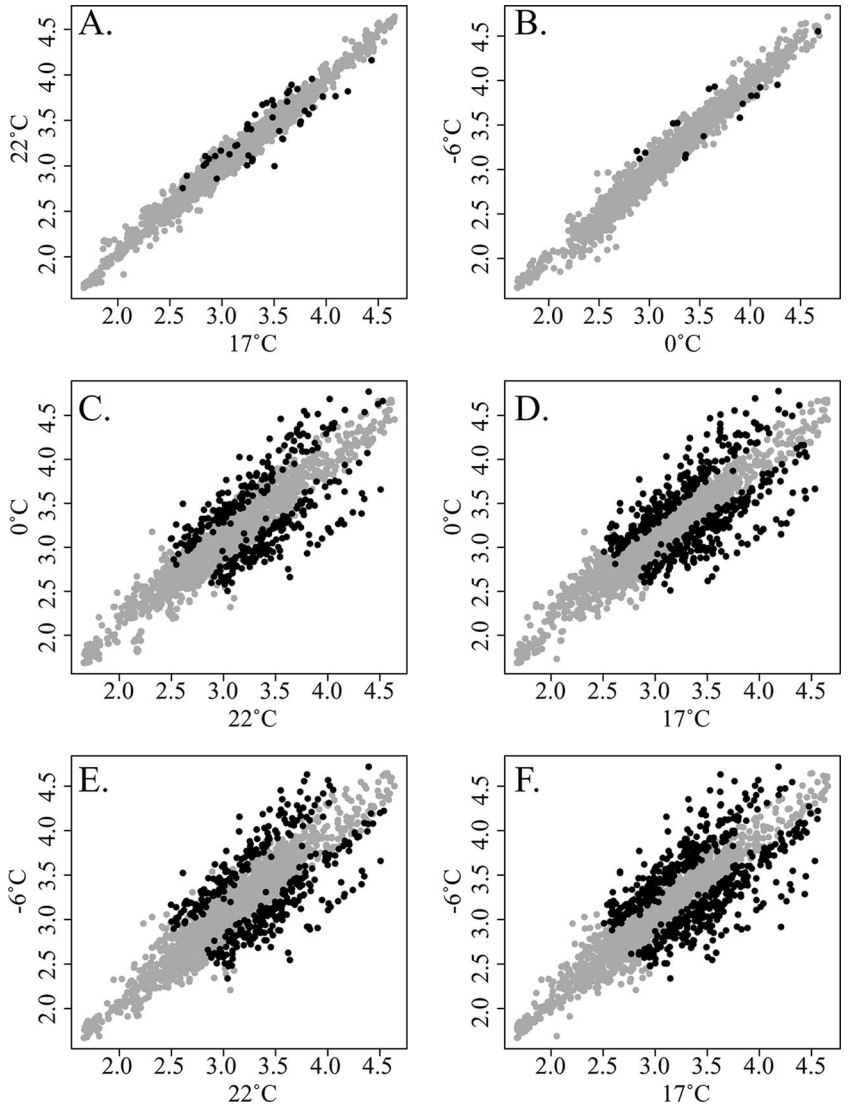

FIG. 2. Log_{10}-transformed normalized average fluorescence values for RNA samples at each temperature ($n = 5$). Values were averaged for five biological replicates at each temperature. Black circles indicate data that are statistically significant ($P < 0.01$) with at least a 1.7-fold change in gene expression and average fluorescence greater than 512 fluorescence units.

simplicity, all changes are expressed relative to the expression levels at T_{opt} (17°C) unless otherwise noted.

Examination of expression by functional category showed that transcription factors, inorganic ion transport and metabolism, and hypothetical and conserved hypothetical proteins were generally upregulated at low temperature (Fig. 3, bars K, P, R, and S). The nucleotide uptake and biosynthesis, energy conversion, ribosomal protein, and amino acid uptake and biosynthesis functional categories were generally downregulated at low temperature (Fig. 3, bars C, J, F, and E). Hypothetical and conserved hypothetical genes accounted for 28% of the differentially expressed transcripts (Fig. 3, bars R and S).

The transcriptome data were also examined for exchange of isozyme expression over temperature, where transcription of one or more members of an isozyme set increased at low temperature while transcription of its partner(s) decreased over temperature. Eleven sets of putative temperature-adapted isozymes were detected in the ANOVA. For the following sets of isozymes there were high confidence annotations for all members of the set (Fig. 4): enzymes for acetyl coenzyme A production, aconitase, D-alanyl-D-alanine carboxypeptidases (DD-peptidases), and DEAD-box RNA helicases.

Substrate uptake and activation. At low temperatures, we observed concurrent twofold upregulation of acetyl-coenzyme A synthetase (Psyc_0821) and downregulation of acetate kinase (Psyc_0197) and phosphotransacetylase (Psyc_0196), two possible pathways of acetate activation (Fig. 4A). Likewise, there was concurrent upregulation of glutamate dehydrogenase and downregulation of glutamate synthase subunits, which are two alternative pathways of ammonium incorporation, at low temperatures (Table 1). Transporters for the uptake of ammonium (Psyc_2044) and inorganic phosphate uptake transporters (Psyc_1926 to Psyc_1930) were not detected as differentially expressed transporters at low temperatures.

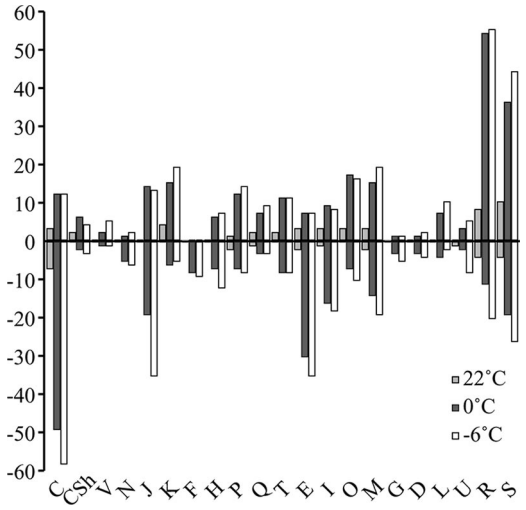

FIG. 3. Numbers of differentially expressed genes at −6°C, 0°C, and 22°C compared with 17°C for COG functional categories. The data for upregulated genes are above the line, and the data for downregulated genes are below the line. C, energy conversion; CSh, previously reported cold shock genes; V, defense mechanisms; N, cell motility; J, translation, ribosomal structure, and biogenesis; K, transcription; F, nucleotide transport and metabolism; H, coenzyme transport and metabolism; P, inorganic ion transport and metabolism; Q, secondary metabolite biosynthesis, transport, and metabolism; T, signal transduction; E, amino acid transport and metabolism; I, lipid transport and metabolism; O, posttranslational modification, protein turnover, and chaperones; M, cell wall, membrane, and envelope biogenesis; G, carbohydrate transport and metabolism; D, cell cycle control, cell division, and chromosome partitioning; L, DNA replication, recombination, and repair; U, intracellular trafficking, secretion, and vesicular transport; R, conserved hypothetical proteins; S, hypothetical proteins.

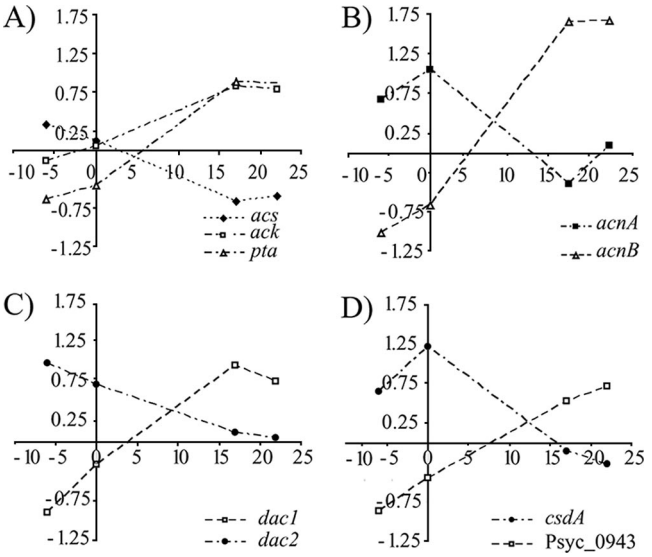

FIG. 4. Exchange of gene expression (vertical axis) over temperature (°C, horizontal axis). Filled symbols indicate data for genes upregulated at low temperature, and open symbols indicate data for genes upregulated at high temperature. The expression values are the $\log_2$-transformed temperature effect estimates from the ANOVA. (A) Acetate activation pathways. (B) Aconitase. (C) DD-Peptidase. (D) ATP-dependent DEAD-box RNA helicase. A total of 11 pairs of homologous genes were found to switch expression with temperature. The genes included have high confidence annotations in the *P. arcticus* 273-4 genome database.

Psyc_1070, encoding the periplasmic subunit for an ABC sulfate transporter, and Psyc_2041, encoding the sulfate uptake transporter and located within the *isc* operon in *P. arcticus*, were upregulated 2.1-fold and 2.3-fold, respectively, at −6°C.

Energy conversion and metabolism. All NADH dehydrogenase, ATP synthase, and Na^+-translocating NADH-ubiquinone oxidoreductase subunits were downregulated four- to eightfold at low temperatures (Fig. 5A). Psyc_1515, encoding cytochrome *bd* ubiquinol oxidase, was upregulated at low temperature with 1.8-fold induction. All tricarboxylic acid cycle and glyoxylate shunt genes were downregulated in the cold, except for the aconitase gene (see data for oxidative stress below) (Fig. 5A). For the genes indicated above, the median R^2 for expression over temperature was 0.93.

mRNA and protein turnover. Twelve peptidases and five RNases were upregulated at low temperatures at least twofold (median R^2, −0.91) (Fig. 5B). Genes for targeting RNAs for degradation were upregulated at low temperatures, including *pcnB*, which was upregulated twofold. Only two RNases were downregulated at 0°C and −6°C: the RNase encoded by Psyc_0292, a cold shock RNA binding domain-containing RNase (downregulated 2.1-fold at −6°C), and polynucleotide phosphorylase (PNPase) (downregulated 1.8-fold at −6°C).

Oxidative stress response. The oxidative stress response was induced at low temperatures (Fig. 5C). In *P. arcticus*, this included induction of genes encoding an ABC transporter for zinc uptake (Psyc_2033 to Psyc_2035), *ahpC*, *hsp33*, the *isc* operon (Psyc_1477 to Psyc_1482), and genes encoding peptide methionine sulfoxide reductases (Psyc_1043 and Psyc_1950) (median R^2, −0.96). Genes for Fe^{2+} uptake transporters, Psyc_1546 and Psyc_1547, were downregulated, consistent with the oxidative stress responses. Likewise, a homolog of the peroxide-resistant aconitase A was upregulated 2.2-fold at −6°C, whereas aconitase B was downregulated 5.6-fold at −6°C (Fig. 4B). A third possible aconitase, encoded by Psyc_1112, was not detected as a differentially expressed enzyme at the different temperatures.

Responses of genes involved in membrane lipid and cell wall synthesis. Fatty acid biosynthesis pathways were downregulated at low temperatures (Fig. 5D) (median R^2, 0.95). Only acyl carrier protein, encoded by Psyc_0522, was upregulated 3.8-fold at −6°C, indicating that this central protein in fatty acid chain growth may require compensation. Genes for fatty acid modification were upregulated at low temperature, including the genes encoding fatty acid desaturase (upregulated 2.7-fold) and cyclopropane fatty acid synthase (upregulated 2.8-fold). The phosphatidylserine decarboxylase gene, Psyc_1925, which encodes phosphatidylethanolamine biosynthesis, was upregulated 3.5-fold at −6°C.

Peptidoglycan biosynthesis genes for murein disaccharides, biosynthetic transglycosylation reactions, and transpeptidation of peptidoglycan strands were downregulated (Fig. 5D) (median R^2, 0.91). In contrast, genes for autolytic breakdown of peptidoglycan, including genes encoding soluble and membrane-bound lytic transglycosylases, Psyc_1272 and Psyc_1273, were upregulated at −6°C.

Expression of genes encoding two putative DD-peptidase

TABLE 1. Amino acid biosynthesis genes that are differentially expressed ($P < 0.01$)[a]

Amino acid(s)	ORF	Gene	Annotation	Change (fold)[b]		
				22°C	0°C	−6°C
Arg	Psyc_0815	*carA*	Putative carbamoyl-phosphate synthase, small subunit	−1.13	−2.46	−3.27
	Psyc_0814	*carB*	Carbamoyl-phosphate synthase, large subunit	−1.25	−3.12	−3.29
	Psyc_0957	*argF*	Probable ornithine carbamoyltransferase	−0.98	−1.84	−1.79
Glu	Psyc_1062	*gdh*	Probable bacterial NAD-specific glutamate dehydrogenase	−1.06	2.14	2.03
	Psyc_1873		Putative glutamate synthase (NADPH dependent), small subunit	−1.20	−1.96	−1.92
	Psyc_1874		Putative glutamate synthase (NADPH dependent), large chain	−1.37	−1.84	−1.91
Gly	Psyc_0798	*gcvP*	Glycine cleavage H protein	−1.24	−3.05	−3.23
	Psyc_0796	*gcvH*	Glycine dehydrogenase	−1.15	−2.46	−3.07
	Psyc_0799	*gcvT*	Putative glycine cleavage T protein (aminomethyl transferase)	1.09	−1.34	−1.42
Ile, Leu,Val	Psyc_0951	*ilvA*	Probable threonine dehydratase I	−1.29	−2.16	−2.62
	Psyc_0527	*ilvG*	Putative acetolactate synthase, large subunit	−1.16	−2.73	−2.87
	Psyc_0528	*ilvM*	Putative acetolactate synthase, small subunit	−1.25	−2.57	−2.77
	Psyc_0529	*ilvC*	Ketol-acid reductoisomerase	−1.21	−2.16	−2.30
Leu	Psyc_1410	*leuB*	3-Isopropylmalate dehydrogenase	−1.21	−2.36	−2.28
	Psyc_1413	*leuC*	3-Isopropylmalate dehydratase, large subunit	−1.35	−2.20	−2.01
	Psyc_1412	*leuD*	3-Isopropylmalate dehydratase, small subunit	−1.27	−2.11	−2.08
Lys	Psyc_0028	*dapB*	Probable dihydrodipicolinate reductase	−1.27	−1.83	−2.38
	Psyc_1523	*asd*	Putative aspartate semialdehyde dehydrogenase	−1.16	−2.17	−2.66
	Psyc_0200	*dapF*	Probable diaminopimelate epimerase	1.06	1.42	1.45
Pro	Psyc_1391	*ocd*	Possible ornithine cyclodeaminase	−1.30	1.44	1.27
	Psyc_0293	*proA*	Putative gamma-glutamyl phosphate reductase	1.01	2.19	2.41
Trp	Psyc_0973	*trpG*	Probable anthranilate phosphoribosyl transferase	1.28	1.33	1.48
	Psyc_0974	*trpD*	Putative anthranilate synthase component II	1.36	1.33	1.52

[a] The genes included are significantly differentially expressed during growth at one or more temperatures.
[b] The data are expressed as changes compared to the results for 17°C.

isozymes, which control peptidoglycan cross-linking frequency, was apparently exchanged between low- and high-temperature transcriptomes. The amino acid sequences encoded by Psyc_0704 (*dac2*) and Psyc_0687 (*dac1*) are 27% identical and 50% similar from amino acid positions 42 to 273 of *dac1* as determined by use of BLAST homology searches against the genome (1). *dac2* aligns with the Pfam database DD-peptidase domain model with an E value of 1.7×10^{-35}. *dac1* aligns with the same model with an E value of 2.1×10^{-87}. *dac2* was upregulated 1.9-fold at −6°C, and *dac1* was downregulated 3.2-fold at −6°C (Fig. 4C).

Amino acid biosynthesis. One of the regulator genes, a *relA* homolog, was upregulated twofold at −6°C compared with 17°C (Fig. 5E), suggesting that *P. arcticus* may respond to deficits in amino-acyl tRNAs (23). Genes for the biosynthesis of proline, methionine, histidine, and tryptophan were upregulated during low-temperature growth (Table 1). Genes for the biosynthesis of branched-chain amino acids, arginine, and lysine were downregulated in cold conditions. The glycine cleavage system genes *gcvH* and *gcvP* were downregulated threefold at low temperature. The differential expression of amino-acyl tRNA synthetases also suggested that cytoplasmic pools of amino acids are different for low-temperature and high-temperature growth (Table 2).

Compatible solute uptake and biosynthesis. In addition to genes encoding proline, glutamate, and glycine biosynthesis, *P. arcticus* also contains genes for the biosynthesis and uptake of carnitine, betaine, and choline. Psyc_0728, encoding choline dehydrogenase, was upregulated 2.1-fold at 22°C, and Psyc_0729, encoding betaine aldehyde dehydrogenase, was upregulated 2.3-fold at 22°C and downregulated 1.4-fold at −6°C. The *P. arcticus* genome contains genes encoding three annotated betaine-carnitine-choline-type transporters; Psyc_0727 was not detected as a gene that is differentially expressed with temperature, Psyc_0826 was downregulated 1.5-fold at −6°C, and Psyc_1301 was upregulated 1.8-fold at −6°C.

Protein folding response. Peptidyl-prolyl *cis-trans* isomerases, trigger factor, and the major heat shock-associated chaperones were downregulated or not detected as differentially expressed molecules at 22°C, 0°C, and −6°C (Table 3). Only chaperones associated with iron-sulfur cluster biosynthesis, oxidative protein damage, and a *clpB* chaperone homolog were upregulated at low temperatures (Fig. 5C and Table 3).

Cold acclimation and cold shock gene expression. *P. arcticus* possesses two major cold shock protein homologs. One *cspA* homolog, Psyc_0531, was expressed at high levels at all temperatures. The gene encoding the other cold shock protein, Psyc_0942, and the adjacent DEAD-box helicase gene, Psyc_0943, were downregulated 3.1-fold and 2.4-fold, respectively, at −6°C. The gene encoding a second DEAD-box helicase, Psyc_1082, was upregulated twofold at low temperatures (Fig. 4D).

The products of Psyc_1082 (*csdA*) and Psyc_0943 are annotated as homologous ATP-dependent DEAD-box RNA heli-

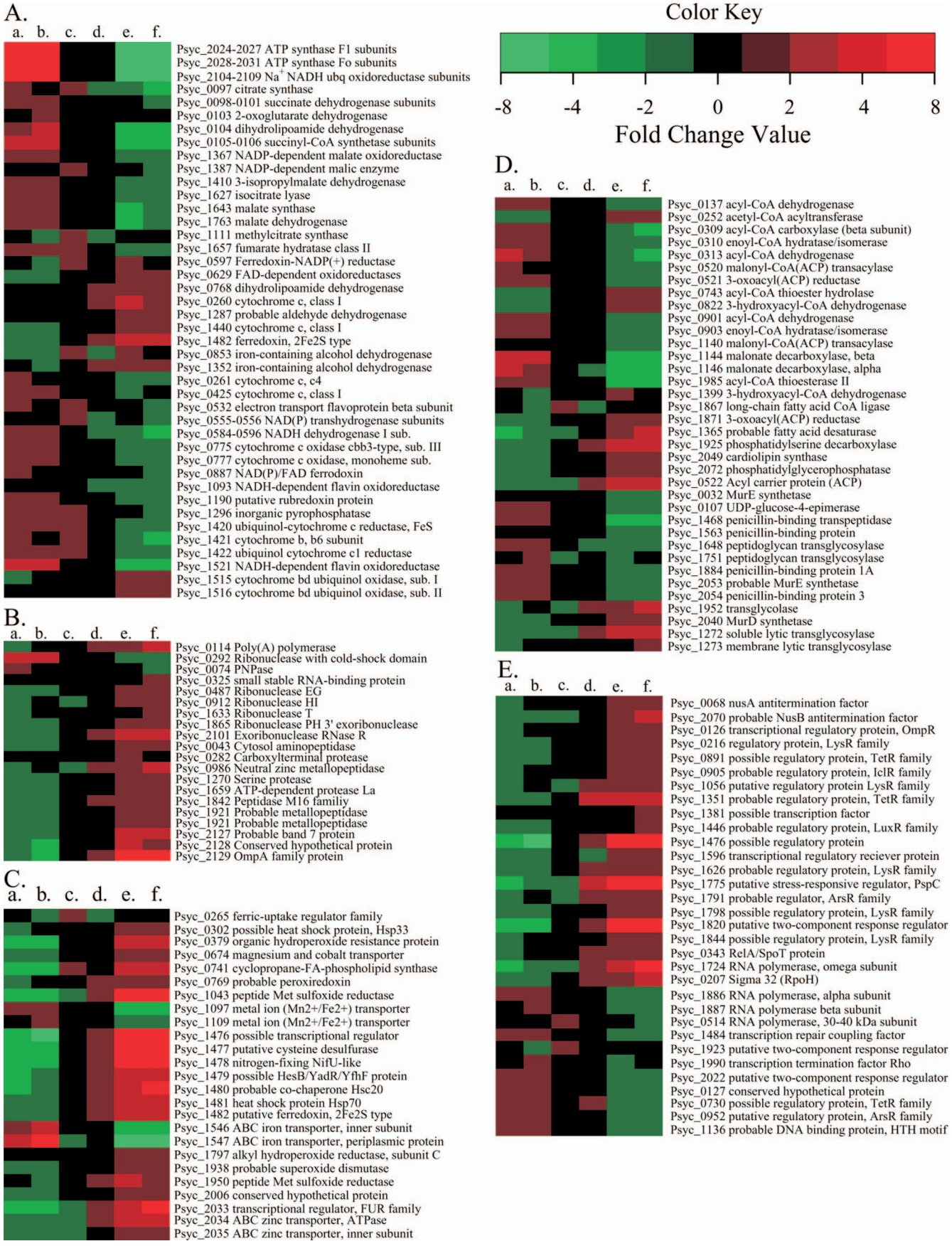
A.
a. b. c. d. e. f.
Psyc_2024-2027 ATP synthase F1 subunits
Psyc_2028-2031 ATP synthase Fo subunits
Psyc_2104-2109 Na+ NADH ubq oxidoreductase subunits
Psyc_0097 citrate synthase
Psyc_0098-0101 succinate dehydrogenase subunits
Psyc_0103 2-oxoglutarate dehydrogenase
Psyc_0104 dihydrolipoamide dehydrogenase
Psyc_0105-0106 succinyl-CoA synthetase subunits
Psyc_1367 NADP-dependent malate oxidoreductase
Psyc_1387 NADP-dependent malic enzyme
Psyc_1410 3-isopropylmalate dehydrogenase
Psyc_1627 isocitrate lyase
Psyc_1643 malate synthase
Psyc_1763 malate dehydrogenase
Psyc_1111 methylcitrate synthase
Psyc_1657 fumarate hydratase class II
Psyc_0597 Ferredoxin-NADP(+) reductase
Psyc_0629 FAD-dependent oxidoreductases
Psyc_0768 dihydrolipoamide dehydrogenase
Psyc_0260 cytochrome c, class I
Psyc_1287 probable aldehyde dehydrogenase
Psyc_1440 cytochrome c, class I
Psyc_1482 ferredoxin, 2Fe2S type
Psyc_0853 iron-containing alcohol dehydrogenase
Psyc_1352 iron-containing alcohol dehydrogenase
Psyc_0261 cytochrome c, c4
Psyc_0425 cytochrome c, class I
Psyc_0532 electron transport flavoprotein beta subunit
Psyc_0555-0556 NAD(P) transhydrogenase subunits
Psyc_0584-0596 NADH dehydrogenase I sub.
Psyc_0775 cytochrome c oxidase cbb3-type, sub. III
Psyc_0777 cytochrome c oxidase, monoheme sub.
Psyc_0887 NAD(P)/FAD ferrodoxin
Psyc_1093 NADH-dependent flavin oxidoreductase
Psyc_1190 putative rubredoxin protein
Psyc_1296 inorganic pyrophosphatase
Psyc_1420 ubiquinol-cytochrome c reductase, FeS
Psyc_1421 cytochrome b, b6 subunit
Psyc_1422 ubiquinol cytochrome c1 reductase
Psyc_1521 NADH-dependent flavin oxidoreductase
Psyc_1515 cytochrome bd ubiquinol oxidase, sub. I
Psyc_1516 cytochrome bd ubiquinol oxidase, sub. II
B.
a. b. c. d. e. f.
Psyc_0114 Poly(A) polymerase
Psyc_0292 Ribonuclease with cold-shock domain
Psyc_0074 PNPase
Psyc_0325 small stable RNA-binding protein
Psyc_0487 Ribonuclease EG
Psyc_0912 Ribonuclease HI
Psyc_1633 Ribonuclease T
Psyc_1865 Ribonuclease PH 3' exoribonuclease
Psyc_2101 Exoribonuclease RNase R
Psyc_0043 Cytosol aminopeptidase
Psyc_0282 Carboxylterminal protease
Psyc_0986 Neutral zinc metallopeptidase
Psyc_1270 Serine protease
Psyc_1659 ATP-dependent protease La
Psyc_1842 Peptidase M16 familiy
Psyc_1921 Probable metallopeptidase
Psyc_1921 Probable metallopeptidase
Psyc_2127 Probable band 7 protein
Psyc_2128 Conserved hypothetical protein
Psyc_2129 OmpA family protein
C.
a. b. c. d. e. f.
Psyc_0265 ferric-uptake regulator family
Psyc_0302 possible heat shock protein, Hsp33
Psyc_0379 organic hydroperoxide resistance protein
Psyc_0674 magnesium and cobalt transporter
Psyc_0741 cyclopropane-FA-phospholipid synthase
Psyc_0769 probable peroxiredoxin
Psyc_1043 peptide Met sulfoxide reductase
Psyc_1097 metal ion (Mn2+/Fe2+) transporter
Psyc_1109 metal ion (Mn2+/Fe2+) transporter
Psyc_1476 possible transcriptional regulator
Psyc_1477 putative cysteine desulfurase
Psyc_1478 nitrogen-fixing NifU-like
Psyc_1479 possible HesB/YadR/YfhF protein
Psyc_1480 probable co-chaperone Hsc20
Psyc_1481 heat shock protein Hsp70
Psyc_1482 putative ferredoxin, 2Fe2S type
Psyc_1546 ABC iron transporter, inner subunit
Psyc_1547 ABC iron transporter, periplasmic protein
Psyc_1797 alkyl hydroperoxide reductase, subunit C
Psyc_1938 probable superoxide dismutase
Psyc_1950 peptide Met sulfoxide reductase
Psyc_2006 conserved hypothetical protein
Psyc_2033 transcriptional regulator, FUR family
Psyc_2034 ABC zinc transporter, ATPase
Psyc_2035 ABC zinc transporter, inner subunit
Color Key
-8 -4 -2 0 2 4 8
Fold Change Value
D.
a. b. c. d. e. f.
Psyc_0137 acyl-CoA dehydrogenase
Psyc_0252 acetyl-CoA acyltransferase
Psyc_0309 acyl-CoA carboxylase (beta subunit)
Psyc_0310 enoyl-CoA hydratase/isomerase
Psyc_0313 acyl-CoA dehydrogenase
Psyc_0520 malonyl-CoA(ACP) transacylase
Psyc_0521 3-oxoacyl(ACP) reductase
Psyc_0743 acyl-CoA thioester hydrolase
Psyc_0822 3-hydroxyacyl-CoA dehydrogenase
Psyc_0901 acyl-CoA dehydrogenase
Psyc_0903 enoyl-CoA hydratase/isomerase
Psyc_1140 malonyl-CoA(ACP) transacylase
Psyc_1144 malonate decarboxylase, beta
Psyc_1146 malonate decarboxylase, alpha
Psyc_1985 acyl-CoA thioesterase II
Psyc_1399 3-hydroxyacyl-CoA dehydrogenase
Psyc_1867 long-chain fatty acid CoA ligase
Psyc_1871 3-oxoacyl(ACP) reductase
Psyc_1365 probable fatty acid desaturase
Psyc_1925 phosphatidylserine decarboxylase
Psyc_2049 cardiolipin synthase
Psyc_2072 phosphatidylglycerophosphatase
Psyc_0522 Acyl carrier protein (ACP)
Psyc_0032 MurE synthetase
Psyc_0107 UDP-glucose-4-epimerase
Psyc_1468 penicillin-binding transpeptidase
Psyc_1563 penicillin-binding protein
Psyc_1648 peptidoglycan transglycosylase
Psyc_1751 peptidoglycan transglycosylase
Psyc_1884 penicillin-binding protein 1A
Psyc_2053 probable MurE synthetase
Psyc_2054 penicillin-binding protein 3
Psyc_1952 transglycolase
Psyc_2040 MurD synthetase
Psyc_1272 soluble lytic transglycosylase
Psyc_1273 membrane lytic transglycosylase
E.
a. b. c. d. e. f.
Psyc_0068 nusA antitermination factor
Psyc_2070 probable NusB antitermination factor
Psyc_0126 transcriptional regulatory protein, OmpR
Psyc_0216 regulatory protein, LysR family
Psyc_0891 possible regulatory protein, TetR family
Psyc_0905 probable regulatory protein, IclR family
Psyc_1056 putative regulatory protein LysR family
Psyc_1351 probable regulatory protein, TetR family
Psyc_1381 possible transcription factor
Psyc_1446 probable regulatory protein, LuxR family
Psyc_1476 possible regulatory protein
Psyc_1596 transcriptional regulatory reciever protein
Psyc_1626 probable regulatory protein, LysR family
Psyc_1775 putative stress-responsive regulator, PspC
Psyc_1791 probable regulator, ArsR family
Psyc_1798 possible regulatory protein, LysR family
Psyc_1820 putative two-component response regulator
Psyc_1844 possible regulatory protein, LysR family
Psyc_0343 RelA/SpoT protein
Psyc_1724 RNA polymerase, omega subunit
Psyc_0207 Sigma 32 (RpoH)
Psyc_1886 RNA polymerase, alpha subunit
Psyc_1887 RNA polymerase beta subunit
Psyc_0514 RNA polymerase, 30-40 kDa subunit
Psyc_1484 transcription repair coupling factor
Psyc_1923 putative two-component response regulator
Psyc_1990 transcription termination factor Rho
Psyc_2022 putative two-component response regulator
Psyc_0127 conserved hypothetical protein
Psyc_0730 possible regulatory protein, TetR family
Psyc_0952 putative regulatory protein, ArsR family
Psyc_1136 probable DNA binding protein, HTH motif

TABLE 2. tRNA synthetase genes that are differentially expressed ($P < 0.01$)[a]

Amino acid	ORF	tRNA synthetase	Change (fold)[b]		
			22°C	0°C	−6°C
Gln	Psyc_0694	Glutaminyl-tRNA synthetase	−1.06	1.68	1.58
Gly	Psyc_1774	Glycyl-tRNA synthetase, alpha subunit	1.32	1.46	1.67
Gly	Psyc_1773	Glycyl-tRNA synthetase, beta subunit	1.40	1.39	1.89
Tyr	Psyc_1970	Tyrosyl-tRNA synthetase	−1.53	−3.89	−5.46
Phe	Psyc_1995	Phenylalanyl-tRNA synthetase, beta subunit	−1.36	−2.97	−3.94
Phe	Psyc_1996	Phenylalanyl-tRNA synthetase, alpha subunit	−1.31	−2.36	−2.99
Cys	Psyc_1361	Cysteinyl-tRNA synthetase, class Ia	−1.21	−1.60	−2.35
Trp	Psyc_1568	Tryptophanyl-tRNA synthetase, class Ib	−1.27	−1.78	−2.17
Ala	Psyc_1460	Alanyl-tRNA synthetase, class IIc	−1.37	−2.38	−2.46
Pro	Psyc_0429	Prolyl-tRNA synthetase, class IIa	−1.20	−1.93	−2.20
Ile	Psyc_0364	Isoleucyl-tRNA synthetase, class Ia	−1.01	−1.71	−1.84
Ser	Psyc_1618	Seryl-tRNA synthetase, class IIa	−1.15	−1.68	−1.43
His	Psyc_0683	Histidyl-tRNA synthetase, class IIa	−1.04	−1.59	−1.33
Arg	Psyc_1946	Arginyl-tRNA synthetase	1.15	−1.42	−1.17
Met	Psyc_1432	Methionyl-tRNA synthetase	−1.09	−1.04	1.06

[a] The genes included are genes that are significantly differentially expressed during growth at one or more temperatures.
[b] The data are expressed as changes compared to the results for 17°C.

cases with high scoring alignments with the TIGRfam DEAD-box helicase equivalog, and these genes are predicted to encode proteins with 396 and 567 amino acids, respectively. CsdA has a C-terminal extension rich in glycine, serine, and arginine, supporting its function at low temperature similar to the function of mesophilic and psychrophilic cold-associated DEAD-box helicases (28). BLAST alignment of amino acid sequences encoded by the two genes yielded 40% identity over an alignment of a 375-amino-acid homologous region which included the DEAD-box RNA helicase domain of each gene product.

Transcription and translation factors associated with cold shock in mesophiles were observed to be upregulated at −6°C and included *rbfA* encoding a ribosomal binding factor (upregulated 1.8-fold), *nusB* and *nusA* (upregulated 1.7-fold and 2.6-fold, respectively), and translation initiation factor IF-2 (upregulated 1.8-fold) (Fig. 5E). However, no previously reported cold shock-associated genes involved in recombination or carbon catabolism were upregulated in the cold.

Comparison of proteome and transcriptome data. We also analyzed how the transcriptome of *P. arcticus* correlated with its proteome using 20 protein spots that displayed an increase in relative abundance during growth at one of the temperature extremes (−6°C or 22°C) (see Table S2 in the supplemental material). The identified proteins (see Table S3 in the supplemental material) represented a range of cellular processes from translation, amino acid synthesis, and cell wall degradation to unknown functions. Of 9 protein spots with increased relative abundance at −6°C, 55% displayed the same expression profile as their transcripts. Similarly, about 50% of 10 protein spots with increased relative abundance at 22°C displayed the same expression profile as their transcripts.

Primary structure disorder prediction. *P. arcticus* possesses two open reading frames (ORFs) annotated as ORFs that encode DD-peptidase and two ORFs annotated as ORFs that encode DEAD-box RNA helicase. Interestingly, both pairs of ORFs contained one member upregulated during growth at T_{opt}, while the other was upregulated during low-temperature growth (Fig. 4C and D). While it is possible that loci upregulated at low temperatures and loci upregulated at T_{opt} have somewhat different substrates, we hypothesized that ORFs upregulated at low temperatures would have greater predicted disorder than their homologues upregulated at T_{opt}. Primary structure disorder was predicted using DisEMBL 1.5 with the default parameters by manually aligning the DisEMBL output to account for gaps in BLAST alignment of the DD-peptidase and DEAD-box helicase ORFs (33).

DisEMBL predicted a coil of 64 amino acid residues near the N-terminal end of the DD-peptidase domain encoded by cold-upregulated *dac2* that is not present in the enzyme encoded by *dac1*. Two additional coils are predicted in the DD-peptidase domain of the enzyme encoded by *dac2*, which are not present in the enzyme encoded by *dac1*, at positions 210 to 225 and positions 354 to 361 in the aligned disorder data. In total, the enzyme encoded by *dac2* contained 155 disordered amino acid residues in the aligned sequence region, whereas the enzyme encoded by *dac1* contained only 128 disordered amino acid residues. Only 32 *dac1*-encoded amino acid positions were predicted to be in hot loops (i.e., highly disordered amino acid positions) in the aligned region, but DisEMBL

FIG. 5. Heat map of selected differentially expressed genes. (A) Energy metabolism genes. (B) Genes encoding RNases and peptidases. (C) Oxidative stress response genes. (D) Fatty acid and cell wall metabolism genes. (E) Genes encoding transcription factors. The results of temperature comparisons are shown in columns, as follows: column a, 22°C versus −6°C; column b, 22°C versus 0°C; column c, 22°C versus 17°C; column d, 0°C versus −6°C; column e, 0°C versus 17°C; column f, −6°C versus 17°C. The data for genes are shown in rows. Values are expressed as fold changes. All genes were differentially expressed in at least one contrast with $P < 0.01$. CoA, coenzyme A; FAD, flavin adenine dinucleotide; ACP, acyl carrier protein; HTH, helix-turn-helix.

TABLE 3. Expression profiles of *P. arcticus* genes involved in protein folding and disaggregation

ORF	Gene	Annotation	Change (fold)[a]		
			22°C	0°C	−6°C
Psyc_0034	*dsbB*	Possible disulfide bond formation protein	1.27	1.41[b]	1.67[b]
Psyc_0254	*dsbC*	Possible thiol:disulfide interchange protein	1.27	1.26	1.56[b]
Psyc_1560	*dsbE*	Probable periplasmic protein thiol:disulfide oxidoreductase DsbE	−1.12	−2.27[b]	−2.14[b]
Psyc_0552	*groES*	Putative chaperonin Hsp10	−1.18	−1.09	−1.41
Psyc_0553	*groEL*	Putative chaperonin Hsp60 family	1.04	1.04	−1.28
Psyc_0027		Probable chaperone protein DnaJ	−1.21	−2.38[b]	−2.33[b]
Psyc_0039	*dnaJ*	Probable heat shock protein DnaJ	−1.01	1.15	1.06
Psyc_2132	*dnaK*	Chaperone protein DnaK	1.19	1.18	1.04
Psyc_2133	*grpE*	Heat shock protein GrpE, Hsp70 family	1.09	−1.16	−1.35[b]
Psyc_0823	*clpB*	Putative chaperonin ClpA/B	1.82[b]	1.40	1.93[b]
Psyc_1941	*clpP*	Putative ATP-dependent ClpP protease, proteolytic subunit	−1.06	−1.06	−1.61[b]
Psyc_1942	*clpX*	Putative ATP-dependent ClpX protease	−1.11	−1.27	−1.66[b]
Psyc_1719	*htpG*	Probable chaperone protein HtpG (Hsp90)	1.07	−1.91[b]	−2.41[b]
Psyc_1940	*tig*	Trigger factor	−1.36	−1.67[b]	−2.22[b]
Psyc_0857		Peptidyl-prolyl isomerase	−1.22	−1.13	−1.09
Psyc_0693	*ppiB*	Peptidyl-prolyl *cis-trans* isomerase, cyclophilin type	−1.29	1.12	−1.58[b]
Psyc_0283	*slyD*	Putative peptidyl-prolyl *cis-trans* isomerase, FKBP type	−1.04	1.08	1.05
Psyc_0358		Probable peptidyl-prolyl *cis-trans* isomerase protein, FKBP type	−1.01	1.10	−1.08
Psyc_1473	*ppiC*	Possible PpiC-type peptidyl-prolyl *cis-trans* isomerase	−1.17	−1.79[b]	−1.67[b]

[a] The data are expressed in changes compared to the results for 17°C.
[b] Significant change ($P < 0.01$).

predicted that 125 amino acids are in hot loops in the *dac2*-encoded enzyme. Thus, much greater overall disorder of the peptide chain is predicted for the cold-upregulated *dac2*-encoded enzyme, consistent not only with the possible higher activity in the cold but also with greater thermolabililty.

DisEMBL predicted two coils in amino acid positions 272 to 336 of the *csdA*-encoded sequence which were not in the Psyc_0943-encoded sequence and another coil in positions 180 to 200 of the aligned sequences. Hot loop predictions by DisEMBL revealed a larger difference in protein disorder over the aligned sequences, with the *csdA*-encoded sequence containing a predicted 120 hot loop amino acid positions, compared with only 70 such positions in the Psyc_0943-encoded sequence. These results are consistent with cold adaptation of *csdA*, the DEAD-box helicase ORF upregulated at −6°C.

Knockout mutants. Knockout mutants with mutations in Psyc_0687 (*dac1*) and Psyc_0704 (*dac2*) were generated to test whether the two gene products preferentially aid growth under cold growth conditions compared with warm growth conditions. We also used knockout mutants with mutations in Psyc_0343, a homolog of the *relA* regulator of the stringent response, a growth rate control regulon that the transcriptome experiment indicated may be induced at low temperature, and of the cold-upregulated DEAD-box helicase (Psyc_1082, *csdA*), to determine if the loss of this gene would result in reduced growth rates at low temperature. Attempts to generate a knockout mutant with a mutation in Psyc_0943 did not result in growth following conjugation when putative conjugants were plated at either T_{opt} or 4°C, suggesting that this gene plays an essential role in growth at these temperatures and preventing further study of a mutant.

Growth curves of mutant strains and the wild type at 22°C, 17°C, 4°C, 0°C, and −2.5°C were analyzed for differences in mutant and wild-type growth parameters. As hypothesized, only the Δ*dac1* strain grew significantly slower than the wild type at T_{opt} (Fig. 6A). At −2.5°C, Δ*relA*, Δ*dac2*, and Δ*csdA* mutants grew slower than the wild type, as predicted from our transcriptome analysis (Fig. 6D) ($P < 0.05$). At 4°C and 0°C only the Δ*csdA* mutant grew significantly more slowly than the wild type (Fig. 6B and C) ($P < 0.05$). Interestingly, mutants predicted to grow poorly in the cold typically grew faster than the wild type at T_{opt} (Fig. 6A) (not statistically significant). The improved growth of the Δ*dac2* mutant compared with the wild type at high temperature coupled with the wild-type growth of the Δ*dac1* mutant at low temperature suggests that the two DD-peptidases may interact competitively. This competition may be relieved by deletion of one participant.

DISCUSSION

Here we report an analysis of a eurypsychrophilic transcriptome during growth at a subzero temperature (21, 22). In the native permafrost environment, the surrounding soil matrix has been permanently frozen for more than 10,000 years, but the microbe and the water layers immediately surrounding it remain liquid and suitable for low-level metabolism (D. Gilichinsky, presented at the Fourth International Symposium on Thermal Engineering and Science for Cold Regions, U.S. Army Cold Regions Research and Engineering Laboratory). Such unfrozen water layers would be enriched in solutes such as salts and organic matter, thus limiting water availability to the cell. *P. arcticus* 273-4 was recently reported to respire and incorporate [^{3}H]leucine in tryptic soy broth containing 2.79 molal NaCl at 4°C (38). While the acetate medium used in the present experiment (containing abundant acetate, ammonium, phosphate, and sea salts) did not explicitly reflect solute pools in the permafrost, this simple nutrient mixture did permit highly reproducible transcriptome analysis by minimizing variability due to culture medium at subzero temperatures and high osmolyte concentrations.

P. arcticus 273-4 exhibits a multifaceted transcriptome response during growth at subzero temperatures. Our results

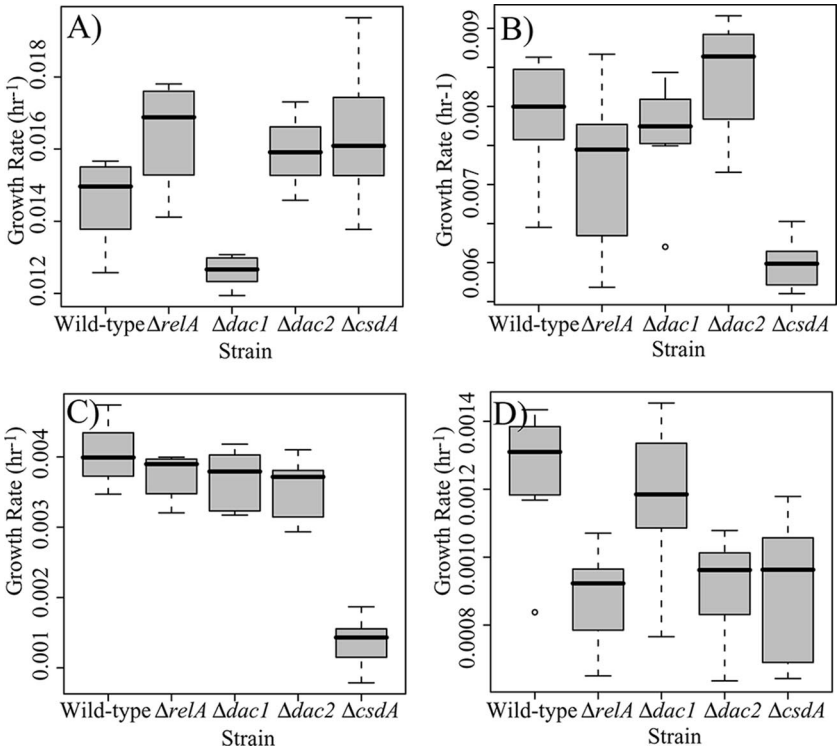

FIG. 6. Growth rate distributions for knockout mutants and wild-type *P. arcticus* controls. The box plots show data for different growth temperatures, as follows: (A) 17°C, (B) 4°C, (C) 0°C, and (D) −2.5°C. Bars indicate the population medians ($n = 8$). Boxes indicate the 25th to 75th percentiles, and whiskers indicate 1.5 times the interquartile range. Outliers are indicated by open circles.

indicate that *P. arcticus* (i) has a cold transcriptome state during growth at temperatures less than 4°C, (ii) downregulates energy metabolism and carbon substrate incorporation genes at low temperature, and (iii) increases the expression of genes for maintenance of membrane, cell wall, and nucleic acid motion but does not upregulate the expression of either RNA or protein chaperones.

Resource efficiency response. Two principal ecological strategies are thought to explain the survival of microbes in permafrost soils that are thousands to millions of years old: (i) a cell can enter a dormant life stage, such as a spore, and thus become resistant to multiple environmental insults, including radiation and desiccation; or ii) a cell must be able to carry out metabolism at a sufficient rate to repair damage due to decay, radiation, desiccation, and the cold. Recent advances in permafrost microbiology suggest that a substantial proportion of the permafrost microbiome is capable of survival, maintenance, and possibly growth metabolic modes in permafrost. It has been argued that slow metabolism and resource conservation at low temperature may be superior to dormancy as a survival strategy over thousands to millions of years in frozen environments (7, 29, 39, 52). The data presented here indicate that *P. arcticus* adopts the slow-metabolism strategy under low-temperature, low-water-activity, and limited-nutrient-availability conditions.

The observed downregulation of energy metabolism, translation, and transcription machinery concurrent with upregulation of RNases, peptidases, *rpoZ*, and *relA* is consistent with responses to limited growth rates and may be indicative of stringent response induction for growth rate control (10). While induction of the stringent response is unclear in *P. arcticus* at low temperature due to a lack of supporting data, such as data from ppGpp assays, a number of strikingly similar gene expression patterns were observed at low temperature, which we interpret to be responses to growth rate limitation at low temperatures. The stringent response is thought to be induced primarily by reduced cytoplasmic pools of charged tRNAs, and changes in amino acid metabolism genes are commonly observed during growth at low temperature. For example, genes for arginine and aromatic amino acid biosynthesis are induced during cold-acclimated growth in *Escherichia coli* and *Bacillus subtilis* at 15°C (8, 36), and arginine biosynthesis and histidine biosynthesis were induced in *Listeria monocytogenes* growing at 10°C (34). *P. arcticus* differentially expressed 42 amino acid biosynthesis and tRNA synthetase genes during growth at low temperature. Indeed, *P. arcticus* growth rates at temperatures less than 0°C were decreased by deletion of the stringent response controller *relA*, and decreased lag phase length and extended reduction in the growth rate in late exponential phase were observed (data not shown), similar to growth phenotypes of Δ*relA* mutants of *B. subtilis* and *E. coli* (16, 49). These combined data suggest that the cytoplasmic pools of glycine, proline, methionine, and tryptophan during growth at temperatures below 0°C may be too small. However, more work is needed to explicitly test the importance of the observed starvation response to growth at low temperatures.

The induction of RNases and peptidases during growth at low temperature is similar to results observed for some meso-

philes. RNase R and PNPase of *E. coli* are induced during cold shock (9, 36). RNase PH, PNPase, and RNase R were induced during cold-acclimated growth of *B. subtilis* (8). PNPase is essential for growth of *Yersinia entercolitica* at low temperature (25). In *P. arcticus*, increased expression of RNases and peptidases during cold-acclimated growth could result in increased turnover of RNA and proteins, probably to conserve biosynthetic precursors during growth with generation times on the order of days or weeks at temperatures where the half-lives of transcripts and peptides are long.

A challenge in the interpretation of functional genomic data during cold-acclimated growth is that the methods assay instantaneous quantities of proteins and transcripts without determining rates of activity of the enzymes. For example, it is likely that *P. arcticus* requires more ATP per generation during low-temperature growth (4), but proteome and transcriptome data show decreased expression of ATP synthase, most likely due to a low instantaneous requirement for ATP in the cell. However, the induction of resource conservation responses in *P. arcticus* is in contrast to results observed for other psychrophiles. *Psychrobacter cryohalolentis* (formerly *Psychrobacter cryopegella*), another species from Siberian permafrost, upregulated energy metabolism enzymes during growth at −4°C in defined acetate medium (5). Increased expression for methanogenesis and methylotrophy were also observed during growth of *Methanococcoides burtonii* at 4°C (24). The *P. arcticus* transcriptome response represents a possible alternative strategy for adjusting central processes for low-temperature growth with basal energy, transcription, and translation machinery that are broadly downregulated under cold conditions.

Maintenance of molecular motion. Among the most well-documented cold-induced genes in bacteria are the genes encoding the major cold shock proteins, DEAD-box RNA helicases, protein chaperones, and membrane fatty acid desaturases that function to maintain disorder in cellular components at decreased temperatures (18, 42). Our results do not support the hypothesis that that there is upregulation of major cold shock proteins or protein chaperones during growth at subzero temperatures, although the product of one *cspA* homolog was highly expressed over the entire growth temperature range.

Cold-inducible DEAD-box helicases are important for unwinding double-stranded RNA during growth at low temperatures in microorganisms (28, 32). We found that the two *P. arcticus* DEAD-box helicase genes were inversely expressed in the two different temperature ranges and that deletion of *csdA* (Psyc_1082) resulted in reduced growth rates at ≤4°C compared to the wild-type growth rates. While the two alleles of the gene encoding RNA helicase may have different target RNA populations, it was clear from deletion of *csdA* that this gene is important for low-temperature growth of *P. arcticus*. The *P. arcticus csdA*-encoded protein also possesses a highly disordered C-terminal extension rich in glycine, serine, and arginine similar to that observed in the psychrophilic methanogen *Methanococcoides burtonii* (32). The similarity of these two cold-adapted RNA helicases in disparate microbes suggests that the disordered C-terminal extension may contribute strongly to psychrophily in polar microbes. It would be interesting to express this allele in mesophiles to test for the capacity to confer low-temperature growth, as was observed in *E. coli* expressing a cold-adapted Cpn60/10 chaperone (46). While the results of recombinant chaperone expression in *E. coli* suggest that protein folding is a major hurdle for low-temperature growth in this species, expression of a psychrophilic enzyme involved in transcript stability during translation could further improve the efficiency of growth at low temperatures and extend the minimum growth temperature of the engineered *E. coli* strain.

While protein misfolding and aggregation are thought to lead to the induction of chaperones and peptidyl-prolyl *cis-trans* isomerases at low temperature (5, 8, 24, 36, 46, 48), only *clpB* and *hsp33* homologs were upregulated in *P. arcticus* during low-temperature growth. Expression of *hsp33* is induced under heat stress and oxidative stress conditions (27), and this *P. arcticus* response is most likely due to increased amounts of reactive oxygen species at low temperature in the culture vessels. This interpretation is corroborated by the induction in *P. arcticus* of an oxidative stress regulon similar to that in *E. coli* (17). The peptide-disaggregating chaperone ClpB is expressed at a high level in *B. subtilis*, *E. coli*, and *L. monocytogenes* at suboptimal temperatures (8, 34, 36). Conservation of *clpB* upregulation in *P. arcticus* indicates that peptide aggregation is a consequence of life in the cold for eurypsychrophiles and mesophiles. However, it is unclear whether compensation of chaperone activity for peptide folding is required by *P. arcticus* at subzero temperatures because *dnaJK*, *groEL/ES*, and the trigger factor were downregulated.

The potential compensation of elasticity loss in the cell wall at low temperature is a new hypothesis resulting from this work. The peptidoglycan cell wall is an elastic structure, and its elasticity is a function of cross bridging between peptidoglycan strands (54). DD-Peptidases control the degree of cross-linking between peptidoglycan strands in the cell wall by catalyzing the removal of one D-alanine residue from peptidoglycan peptides, thus preventing the action of transpeptidase (41). The exchange of expression of two DD-peptidase alleles and the upregulation of lytic tranglycosylases may serve as a means of maintaining elasticity in the cell wall during growth at high osmolyte concentrations and low temperatures.

Conclusion. While transcriptome analyses can provide insight into coarse physiological changes by assaying global changes in gene transcription, they do not take into account translational and posttranslational regulation. Indeed, a small sampling of the *P. arcticus* proteome revealed that only 50% of identified proteins displayed the same expression profile as their transcripts. Similar results were obtained in a combined transcriptome and proteome analysis of *B. subtilis* growing at 15°C, which demonstrated that only 29% of identified proteins displayed the same expression profile as their transcripts (8). Thus, we generally limit our interpretation of transcriptome results to responses requiring the coordinated expression of numerous genes.

The combined transcriptome, knockout mutant data, and proteome data consistently indicate that *P. arcticus* genes for cellular processes as diverse as membrane and peptidoglycan synthesis, energy metabolism, carbon catabolism, nucleotide biosynthesis, amino acid biosynthesis, RNA polymerase, and the ribosome are adapted to function across the growth temperature range of the organism and respond to growth rate limitation rather than directly to low temperature. Compensa-

tion via increased gene expression was reserved for specific processes, such as cell wall and membrane dynamics, differential expression of a small number of isozyme pairs, specific biosynthetic steps in amino acid metabolism, and macromolecular turnover at low temperature. As expected in genome-scale experiments, our results suggest several questions for future research. First, a test of the cell wall elasticity adjustment hypothesis, using the atomic force microscopy method of Yao and colleagues (54), would provide insight into the importance of DD-peptidase exchange over temperature. Second, combination of the data presented here with data from metabolic flux analysis during growth at low temperatures with labeled acetate as a substrate would provide insight into the impact of expression changes on growth physiology at low temperatures (51). Of particular interest would be direct measurement of changes in cytoplasmic amino acid pools with temperature, which we propose limits growth rates (on acetate) at subzero temperatures.

ACKNOWLEDGMENTS

This work was supported by the NASA Astrobiology Institute.

We acknowledge the MSU Research Technology Support Facility for technical services, including microarray printing and proteome analysis. Teresa Bergholz, Lukas Wick, and Weihong Qi provided helpful discussions of microarray analysis techniques.

ADDENDUM IN PROOF

The development of the genetic system for *Psychrobacter arcticus* 273-4 was recently reported in detail by C. Bakermans, R. E. Sloup, D. G. Zarka, M. F. Thomashow, and J. M. Tiedje (Extremophiles **13:**21–30, 2009). Additionally, a recent report examined the transcriptome of a gram-positive permafrost isolate, *Exiguobacterium sibericum* 255-15, over temperatures from −2.5°C to 39°C (D. F. Rodrigues, N. Ivanova, Z. He, M. Hubner, J. Zhou, and J. M. Tiedje, BMC Genomics **9:**547, 2008). Among the many findings, exchange of alpha-amylase isozymes from −2.5°C to 39°C was reported.

REFERENCES

1. **Altschul, S. F., T. L. Madden, A. A. Schaffer, J. Zhang, Z. Zhang, W. Miller, and D. J. Lipman.** 1997. Gapped BLAST and PSI-BLAST: a new generation of protein database search programs. Nucleic Acids Res. **25:**3389–3402.
2. **Angelidis, A. S., L. T. Smith, L. M. Hoffman, and G. M. Smith.** 2002. Identification of *opuC* as a chill-activated and osmotically activated carnitine transporter in *Listeria monocytogenes*. Appl. Environ. Microbiol. **68:**2644–2650.
3. **Bakermans, C., H. L. Ayala-del-Rio, M. A. Ponder, T. Vishnivetskaya, D. Gilichinsky, M. F. Thomashow, and J. M. Tiedje.** 2006. *Psychrobacter cryohalolentis* sp. nov. and *Psychrobacter arcticus* sp. nov., isolated from Siberian permafrost. Int. J. Syst. Evol. Microbiol. **56:**1285–1291.
4. **Bakermans, C., and K. H. Nealson.** 2004. Relationship of critical temperature to macromolecular synthesis and growth yield in *Psychrobacter cryopegella*. J. Bacteriol. **186:**2340–2345.
5. **Bakermans, C., S. L. Tollaksen, C. S. Giometti, C. Wilkerson, J. M. Tiedje, and M. F. Thomashow.** 2007. Proteomic analysis of *Psychrobacter cryohalolentis* K5 during growth at subzero temperatures. Extremophiles **11:**343–354.
6. **Breezee, J., N. Cady, and J. T. Staley.** 2004. Subfreezing growth of the sea ice bacterium "Psychromonas ingrahamii." Microb. Ecol. **47:**300–304.
7. **Brinton, K. L., A. I. Tsapin, D. Gilichinsky, and G. D. McDonald.** 2002. Aspartic acid racemization and age-depth relationships for organic carbon in Siberian permafrost. Astrobiology **2:**77–82.
8. **Budde, I., L. Steil, C. Scharf, U. Volker, and E. Bremer.** 2006. Adaptation of *Bacillus subtilis* to growth at low temperature: a combined transcriptomic and proteomic appraisal. Microbiology **152:**831–853.
9. **Cairrao, F., A. Cruz, H. Mori, and C. M. Arraiano.** 2003. Cold shock induction of RNase R and its role in the maturation of the quality control mediator SsrA/tmRNA. Mol. Microbiol. **50:**1349–1360.
10. **Chang, D. E., D. J. Smalley, and T. Conway.** 2002. Gene expression profiling of *Escherichia coli* growth transitions: an expanded stringent response model. Mol. Microbiol. **45:**289–306.
11. **Christner, B. C.** 2002. Incorporation of DNA and protein precursors into macromolecules by bacteria at −15°C. Appl. Environ. Microbiol. **68:**6435–6438.
12. **Churchill, G. A.** 2004. Using ANOVA to analyze microarray data. BioTechniques **37:**173–175,177.
13. **Cui, X., and G. A. Churchill.** 2003. Statistical tests for differential expression in cDNA microarray experiments. Genome Biol. **4:**210.
14. **Cui, X., J. T. Hwang, J. Qiu, N. J. Blades, and G. A. Churchill.** 2005. Improved statistical tests for differential gene expression by shrinking variance components estimates. Biostatistics **6:**59–75.
15. **Denef, V. J., J. A. Klappenbach, M. A. Patrauchan, C. Florizone, J. L. Rodrigues, T. V. Tsoi, W. Verstraete, L. D. Eltis, and J. M. Tiedje.** 2006. Genetic and genomic insights into the role of benzoate-catabolic pathway redundancy in *Burkholderia xenovorans* LB400. Appl. Environ. Microbiol. **72:**585–595.
16. **Eymann, C., G. Homuth, C. Scharf, and M. Hecker.** 2002. *Bacillus subtilis* functional genomics: global characterization of the stringent response by proteome and transcriptome analysis. J. Bacteriol. **184:**2500–2520.
17. **Farr, S. B., and T. Kogoma.** 1991. Oxidative stress responses in *Escherichia coli* and *Salmonella typhimurium*. Microbiol. Rev. **55:**561–585.
18. **Feller, G.** 2007. Life at low temperatures: is disorder the driving force? Extremophiles **11:**211–216.
19. **Feller, G., and C. Gerday.** 2003. Psychrophilic enzymes: hot topics in cold adaptation. Nat. Rev. Microbiol. **1:**200–208.
20. **Georlette, D., V. Blaise, T. Collins, S. D'Amico, E. Gratia, A. Hoyoux, J. C. Marx, G. Sonan, G. Feller, and C. Gerday.** 2004. Some like it cold: biocatalysis at low temperatures. FEMS Microbiol. Rev. **28:**25–42.
21. **Gilichinsky, D.** 2001. Permafrost model of extraterrestrial habitat, p. 271–295. *In* G. Horneck (ed.), Astrobiology. Springer-Verlag, New York, NY.
22. **Gilichinsky, D., E. Rivkina, V. Shcherbakova, K. Laurinavichuis, and J. M. Tiedje.** 2003. Supercooled water brines within permafrost—an unknown ecological niche for microorganisms: a model for astrobiology. Astrobiology **3:**331–341.
23. **Goldman, E., and H. Jakubowski.** 1990. Uncharged tRNA, protein synthesis, and the bacterial stringent response. Mol. Microbiol. **4:**2035–2040.
24. **Goodchild, A., N. F. Saunders, H. Ertan, M. Raftery, M. Guilhaus, P. M. Curmi, and R. Cavicchioli.** 2004. A proteomic determination of cold adaptation in the Antarctic archaeon, *Methanococcoides burtonii*. Mol. Microbiol. **53:**309–321.
25. **Goverde, R. L., J. H. Huis in't Veld, J. G. Kusters, and F. R. Mooi.** 1998. The psychrotrophic bacterium *Yersinia enterocolitica* requires expression of *pnp*, the gene for polynucleotide phosphorylase, for growth at low temperature (5 degrees C). Mol. Microbiol. **28:**555–569.
26. **Hegde, P., R. Qi, K. Abernathy, C. Gay, S. Dharap, R. Gaspard, J. E. Hughes, E. Snesrud, N. Lee, and J. Quackenbush.** 2000. A concise guide to cDNA microarray analysis. BioTechniques **29:**548–562.
27. **Ilbert, M., J. Horst, S. Ahrens, J. Winter, P. C. Graf, H. Lilie, and U. Jakob.** 2007. The redox-switch domain of Hsp33 functions as dual stress sensor. Nat. Struct. Mol. Biol. **14:**556–563.
28. **Iost, I., and M. Dreyfus.** 2006. DEAD-box RNA helicases in *Escherichia coli*. Nucleic Acids Res. **34:**4189–4197.
29. **Johnson, S. S., M. B. Hebsgaard, T. R. Christensen, M. Mastepanov, R. Nielsen, K. Munch, T. Brand, M. T. Gilbert, M. T. Zuber, M. Bunce, R. Ronn, D. Gilichinsky, D. Froese, and E. Willerslev.** 2007. Ancient bacteria show evidence of DNA repair. Proc. Natl. Acad. Sci. USA **104:**14401–14405.
30. **Junge, K., H. Eicken, and J. W. Deming.** 2003. Motility of *Colwellia psychrerythraea* strain 34H at subzero temperatures. Appl. Environ. Microbiol. **69:**4282–4284.
31. **Kostka, J., and K. H. Nealson.** 1998. Isolation, cultivation and characterization of iron- and manganese-reducing bacteria, p. 55–68. *In* G. Sayler (ed.), Techniques in microbial ecology. Oxford University Press, New York, NY.
32. **Lim, J., T. Thomas, and R. Cavicchioli.** 2000. Low temperature regulated DEAD-box RNA helicase from the Antarctic archaeon, *Methanococcoides burtonii*. J. Mol. Biol. **297:**553–567.
33. **Linding, R., L. J. Jensen, F. Diella, P. Bork, T. J. Gibson, and R. B. Russell.** 2003. Protein disorder prediction: implications for structural proteomics. Structure **11:**1453–1459.
34. **Liu, S., J. E. Graham, L. Bigelow, P. D. Morse II, and B. J. Wilkinson.** 2002. Identification of *Listeria monocytogenes* genes expressed in response to growth at low temperature. Appl. Environ. Microbiol. **68:**1697–1705.
35. **Maki, S., M. Yoneta, and Y. Takada.** 2006. Two isocitrate dehydrogenases from a psychrophilic bacterium, *Colwellia psychrerythraea*. Extremophiles **10:**237–249.
36. **Phadtare, S., and M. Inouye.** 2004. Genome-wide transcriptional analysis of the cold shock response in wild-type and cold-sensitive, quadruple-*csp*-deletion strains of *Escherichia coli*. J. Bacteriol. **186:**7007–7014.
37. **Ponder, M. A., S. J. Gilmour, P. W. Bergholz, C. A. Mindock, R. Hollingsworth, M. F. Thomashow, and J. M. Tiedje.** 2005. Characterization of potential stress responses in ancient Siberian permafrost psychroactive bacteria. FEMS Microbiol. Ecol. **53:**103–115.
38. **Ponder, M. A., M. F. Thomashow, and J. M. Tiedje.** 2008. Metabolic activity of Siberian permafrost isolates, Psychrobacter arcticus and *Exiguobacterium sibiricum*, at low water activities. Extremophiles **12:**481–490.

39. **Price, P. B., and T. Sowers.** 2004. Temperature dependence of metabolic rates for microbial growth, maintenance, and survival. Proc. Natl. Acad. Sci. USA **101:**4631–4636.
40. **Russell, N. J.** 2000. Toward a molecular understanding of cold activity of enzymes from psychrophiles. Extremophiles **4:**83–90.
41. **Scheffers, D. J., and M. G. Pinho.** 2005. Bacterial cell wall synthesis: new insights from localization studies. Microbiol. Mol. Biol. Rev. **69:**585–607.
42. **Scherer, S., and K. Neuhaus.** 2002. Life at low temperatures. *In* M. Dworkin (ed.), The prokaryotes: an evolving electronic resource for the microbiological community, 3rd ed., release 3.9 ed. Springer-Verlag, New York, NY.
43. **Smyth, G. K.** 2004. Linear models and empirical Bayes methods for assessing differential expression in microarray experiments. Stat. Appl. Genet. Mol. Biol. **3:**Article3.
44. **Somero, G. N.** 1995. Proteins and temperature. Annu. Rev. Physiol. **57:**43–68.
45. **Storey, J. D., and R. Tibshirani.** 2003. Statistical significance for genomewide studies. Proc. Natl. Acad. Sci. USA **100:**9440–9445.
46. **Strocchi, M., M. Ferrer, K. N. Timmis, and P. N. Golyshin.** 2006. Low temperature-induced systems failure in *Escherichia coli*: insights from rescue by cold-adapted chaperones. Proteomics **6:**193–206.
47. **Tasara, T., and R. Stephan.** 2006. Cold stress tolerance of *Listeria monocytogenes*: a review of molecular adaptive mechanisms and food safety implications. J. Food Prot. **69:**1473–1484.
48. **Thomashow, M. F.** 1999. Plant cold acclimation: freezing tolerance genes and regulatory mechanisms. Annu. Rev. Plant Physiol. Plant Mol. Biol. **50:**571–599.
49. **Traxler, M. F., S. M. Summers, H. T. Nguyen, V. M. Zacharia, G. A. Hightower, J. T. Smith, and T. Conway.** 2008. The global, ppGpp-mediated stringent response to amino acid starvation in Escherichia coli. Mol. Microbiol. **68:**1128–1148.
50. **Vishnivetskaya, T., S. Kathariou, J. McGrath, D. Gilichinsky, and J. M. Tiedje.** 2000. Low-temperature recovery strategies for the isolation of bacteria from ancient permafrost sediments. Extremophiles **4:**165–173.
51. **Wiechert, W.** 2001. 13C metabolic flux analysis. Metab. Eng. **3:**195–206.
52. **Willerslev, E., A. J. Hansen, and H. N. Poinar.** 2004. Isolation of nucleic acids and cultures from fossil ice and permafrost. Trends Ecol. Evol. **19:**141–147.
53. **Yang, Y. H., and T. P. Speed.** 2002. Design issues for cDNA microarray experiments. Nat. Rev. **3:**579–588.
54. **Yao, X., M. Jericho, D. Pink, and T. Beveridge.** 1999. Thickness and elasticity of gram-negative murein sacculi measured by atomic force microscopy. J. Bacteriol. **181:**6865–6875.